American Journal of Water Science and Engineering
2023; 9(4): 97-107
http://www.sciencepublishinggroup.com/j/ajwse
doi: 10.11648/j.ajwse.20230904.12
ISSN: 2575-1867 (Print); ISSN: 2575-1875 (Online)

Defluoridation of Groundwater by Activated Carbon Derived from Water Hyacinth (*Pontederia crassipes*) by Phosphoric Acid Activation

Eric Mugambi Muchunku*, Peter Kuria Ndiba, Erick Auma Omondi

Department of Civil and Construction Engineering, University of Nairobi, Nairobi, Kenya

Email address:

ericmuchunku@gmail.com (Eric Mugambi Muchunku), pkndiba@uonbi.ac.ke (Peter Kuria Ndiba), omorric@gmail.com (Erick Auma Omondi)

*Corresponding author

To cite this article:

Eric Mugambi Muchunku, Peter Kuria Ndiba, Erick Auma Omondi. Defluoridation of Groundwater by Activated Carbon Derived from Water Hyacinth (*Pontederia crassipes*) by Phosphoric Acid Activation. *American Journal of Water Science and Engineering*. Vol. 9, No. 4, 2023, pp. 97-107. doi: 10.11648/j.ajwse.20230904.12

Received: October 12, 2023; **Accepted**: November 7, 2023; **Published**: November 17, 2023

Abstract: Elevated concentration of fluoride in groundwater poses serious health concerns in communities that depend on the groundwater for their drinking water. Efforts to develop appropriate defluoridation techniques have experienced challenges such as low efficiency, unaffordability, skill shortage, and cultural perceptions. This study evaluated the use of water hyacinth-derived activated carbon as an indigenous, environment-friendly, and socio-economically acceptable alternative technique for defluoridation. Dried water hyacinth stems were impregnated with concentrated phosphoric acid to three times their weight, and then calcinated in a muffle furnace by increasing the temperature at a rate of 5°C /min up to 600°C. The produced WHAC was characterized by scanning electron microscopy (SEM), proximate analysis and Fourier transform infrared (FT-IR) spectroscopy. Batch experiments determined effects of pH, contact time and adsorbent dosage on defluoridation efficiency. The results revealed a bulk density of 0.123 g/cm^3, ash content 8.9% and fixed carbon content 66.7%. These characteristics were comparable to those of selected commercial activated carbons (CACs). The ash content was less than 10% and fixed carbon greater than 65%, suggesting high surface area and porosity that are indicative of a good quality activated carbon. The SEM revealed a rough and irregular texture illustrating high porosity. The WHAC achieved a fluoride removal efficiency of 82.6%, at pH 3 and contact time of 120 min. Fluoride adsorption by WHAC was best described by Freundlich isotherm model with a correlation factor (R^2) of 0.952 and an adsorption intensity (n) of 0.285 that indicated heterogeneity of the WHAC. The adsorption was described by pseudo-second order kinetic model with a correlation factor (R^2) of 0.999 and comparable experimental and theoretical adsorption capacities of 0.4608 and 0.4656, respectively, which suggested chemisorption adsorption of fluoride onto WHAC.

Keywords: Defluoridation, Activated Carbon, Groundwater, Water Hyacinth, Adsorption, Isotherm

1. Introduction

Groundwater quality is of global concern following the growing demand for groundwater occasioned by its widespread distribution and accessibility for domestic and industrial use [41]. Elevated fluoride concentration in groundwater is regarded as both a socio-economic and health concern, particularly for the low-income communities that depend on groundwater as the main source of drinking water [54]. For example, 79% of the total groundwater abstracted in Kenya is used for domestic purposes while 39% of households in rural areas depend on groundwater as the main potable water source [22]. However, the use of groundwater faces the challenge of elevated fluoride concentrations which vary greatly with geographic location. For instance, Lake Nakuru region in Kenya has recorded 2,800 mg/L fluoride concentration [54], one of the highest known fluoride concentrations in the world. Other areas such as Baringo, Narok, Kajiado, Nairobi, and Thika have at least 50% of boreholes containing fluorides above 1.5 mg/L [5]. Groundwater samples from Elementaita have recorded fluoride concentrations ranging between 0.2 and 20.9 mg/L

[21], while Naivasha has reported concentrations in the range of 3.0 to 9.3 mg/L [50].

Although consumption of fluorides in small quantities is essential for bones and teeth preservation, the World Health Organization (WHO) identifies fluoride, arsenic and nitrate as compounds associated with widespread health effects [52]. The exposure to high concentration of fluorides is linked to numerous adverse health effects ranging from moderate dental fluorosis, reduced immunity and heightened risk of bone fractures, to severe crippling fluorosis and weakened respiratory system [15, 45]. Averting such effects necessitates adoption of the WHO guidelines limiting fluoride concentration in potable water to less than 1.5 mg/L. However, in Kenya, the Water Services and Regulatory Board (WASREB) allows for a maximum fluoride concentration of 3 mg/L in exceptional cases, based on local and climatic conditions [51].

To address the challenges of fluoride in groundwater, several natural and artificial water treatment methods such as chemical treatment, membrane separation, electrolysis, electrodialysis, ion exchange, reverse osmosis and adsorption with activated carbon have been used [34]. Nevertheless, most of these defluoridation techniques have a short service life and are unaffordable for decentralized systems that can be adopted by communities in developing countries [43]. Consequently, some defluoridation technologies including the use of alum, the Nalgonda technique, bone char filters, contact precipitation and adsorption by locally made activated carbon, have been studied for their application in decentralized systems [40]. Among these methods, adsorption by activated carbon presents an effective physicochemical method for defluoridation [17].

Activated carbon (AC) is an amorphous, versatile, black, porous material with high surface reactivity and large surface area in the range of 500 to 1500 m^2/g that is capable of defluoridation by adsorption [3]. The AC can be prepared chemically by treatment of carbon rich materials with phosphoric acid (H_3PO_4) or hydroxides of sodium and potassium, followed by pyrolysis at temperatures of 350 to 600ºC in an inert environment [1].

Adsorption involves the diffusion of the dissolved contaminant species to the solid phase surface, and adhesion by weak intermolecular forces. It occurs in three phases namely; external mass transfer, diffusion through the micro pores and intra-particle diffusion [35, 17, 30]. Adhesion of fluoride ions to the surface of AC involves interactions such as ion exchange, hydrogen bonding, acid-base reactions, electrostaticity and complexation reactions with functional moieties like hydroxyl (-OH) and carboxyl (-COOH), present on the AC surface [13, 27].

The efficiency of AC in defluoridation depends on the characteristics of raw water and the adsorbent, including the initial fluoride concentration, temperature, contact time, adsorbent dosage, co-existing ions and pH [24]. On the other hand, the characteristics of the adsorbent, depend on the properties of the precursor used, which influences the quality of AC produced and ultimately, its adsorptive capacity [25]. Generally, any precursor with elementary carbonaceous composition can be used for production of AC. However, a good precursor should have low volatile matter, low organic compounds and large mechanical and thermal resistance [9]. Other factors influencing the choice of a precursor include its availability, ease of desorption and alternatives for sludge disposal [26]. Lignocellulosic biomass from plants presents suitable precursors based on their affordability, renewability and proportions of ash, volatile matter and carbon [18]. Plant materials such as walnut shells, coconut shells, fruit stones, olives, seaweed, and agricultural wastes such as watermelon peel and rice straw, have been used successfully in the production of ACs [53, 7, 10].

Water hyacinth (WH) is a flowering aquatic plant of the Pontederiaceae family that grows on water surfaces, and reproduces by runners. The plant can propagate a hundred-fold in only 23 days, and double its mat size in about 2 weeks, making it invasive to the aquatic ecosystem [8, 11]. The reproductive characteristic of WH qualifies it as a renewable resource with potential for numerous uses including biofuel, fertilizer and as a precursor in AC production [48, 39]. The lignocellulosic properties of WH and its low ash content are consistent with other plant biomasses that have successfully been used for AC production [14]. For example, WH collected from Lake Victoria in Kenya, revealed crude fibre and ash contents of 19.4 and 31.9% of the water hyacinth dry mass, respectively, indicating its suitability for production of quality AC [38]. The use of WH in the production of AC can lower the demand on non-renewable precursors such as coal, lignite and petroleum coke [18]. This study prepared and characterized activated carbon from WH stems, and evaluated its removal of fluoride from water.

2. Materials and Methods

2.1. Sample Collection and Preparation

Water samples were obtained from a borehole in Nakuru at coordinates $0^o10'48"$ S, 35^o 58' 29" E. The samples were collected in plastic containers pre-rinsed with distilled water, at peak water usage and slow pumping rate. Before collection, the borehole system was purged for 20 minutes to remove any stagnant water in the casing. The temperature and pH of the water samples were recorded at the point of collection with the use of a handheld immersion temperature probe and pH meter (Hanna HI 9812). The fluoride concentration was tested at the lab using a high range fluoride meter (Hanna HI 96739) before storage of the samples awaiting defluoridation tests.

Water hyacinth samples were collected from Kisumu Port of Lake Victoria at coordinates 0°09'39.3" S, 34°33'14.6" E. Mature, healthy water hyacinth plants were selected, their leaves and roots cut off and the stems kept for use in preparation of AC. Figure 1 shows the groundwater and water hyacinth sampling locations.

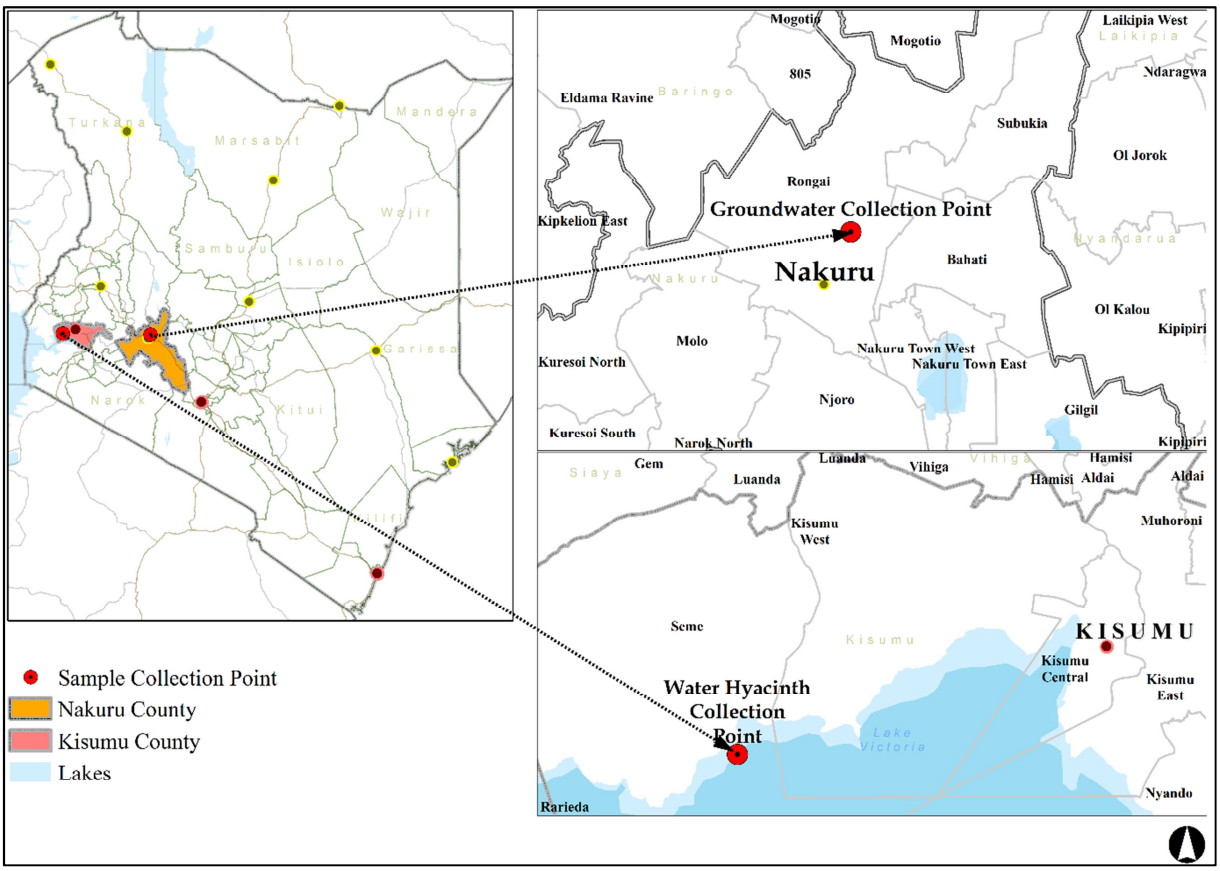

Figure 1. *Groundwater and Water hyacinth sampling points.*

2.2. Preparation of WHAC

Water hyacinth (WH) stems were cleaned using distilled water and then soaked overnight in 0.25M (EDTA) to remove any metal ions on the surfaces. Approximately 15 kg of the stem samples were sun-dried for 3 days and subsequently in a Biobase HAS T50 oven at 110°C for 24 hours to drain excess moisture from the stems. The dry WH stems were impregnated with H_3PO_4 by soaking in H_3PO_4 three times their weight, to introduce chemical functional groups on the surface of the material [19], and then oven dried at 110°C for 48 hours. The dried stems were placed in a muffle furnace and heated gradually at a rate of 5°C /min up to 600°C for 3 hours in the absence of air [53]. The resultant WHAC was cooled to room temperature before cleaning using distilled water to a stable supernatant pH of 6-7. The WHAC was then oven-dried at 110°C for 24 hours before grinding to a size passing 125µm sieve. The powdered WHAC was stored in desiccators awaiting characterization and application in defluoridation experiments.

2.3. Characterization of WHAC

A magnified image of WHAC was obtained using a NeoScope JCM-7000 benchtop scanning electron microscopy (SEM) machine while the chemical composition was determined by Bruker Fourier Transform Infrared Spectroscopy (FT-IR) machine. Proximate analysis was conducted following ASTM D7582-10 method to obtain ash and moisture content, volatile matter and fixed carbon content. The pH of WHAC was obtained by placing 1.0 g of WHAC in 100 mL of distilled water, stirring and then filtering with a glass fiber filter paper and measuring the pH of the filtrate with a Hanna HI 9812 pH meter. The bulk density of WHAC was also determined. The observed characteristics of WHAC were compared with the respective properties of CACs as established from manufacturer's specifications and literature.

2.4. Batch Adsorption Experiments

Batch adsorption tests were undertaken to determine the effect of contact duration, pH and dosage on defluoridation efficiency of WHAC. To establish the influence of pH on adsorption, the pH of the water sample was varied between 3 and 11 using 1M NaOH and HCl, while the WHAC dosage and contact duration were maintained at 0.2 g/100 mL and 120 minutes, respectively. To determine the effect of adsorbent dosage on defluoridation efficiency WHAC dosages between 0.2 and 1.6 g/100 mL were used while maintaining contact time at 120 minutes. The pH of the raw water was modified to the selected pH as established in the previous test. Similarly, to determine the effect of contact time, the pH and adsorbent dosage selected in the previous tests were used while varying contact time between 5 and 180 minutes. The groundwater dosed with WHAC was placed in conical flasks and mixed at 200 rpm using a magnetic stirrer. The solid and liquid phases were separated by filtration using a glass fiber filter paper, and the fluoride concentration measured with Hanna HI 96739

fluoride meter [33]. Fluoride removal efficiencies were computed using equation (1) while the equilibrium fluoride adsorbed by WHAC determined using equation (2).

$$R(\%) = 100 \text{ x } \frac{C_o - C}{C_o} \quad (1)$$

$$q_e = \frac{(C_o - C_e)V}{m} \quad (2)$$

Where; R is the fluoride removal efficiency (%), q_e is the fluoride adsorbed per mass unit of WHAC (mg/g), m is the mass of WHAC (g), V is the volume of the solution (L). and C_0, C and C_e represent initial, final and equilibrium fluoride concentration (mg/L) respectively.

2.5. Adsorption Isotherms

Adsorption isotherms provide a basis for design of adsorption-based treatment systems by providing information on the process equilibrium and the theoretical adsorption capacity for a given pollutant [44]. In this study, the Langmuir and Freundlich isotherm models, equations (3) and (4) respectively, were used because of their simplicity and applicability.

$$\frac{1}{q_e} = \frac{1}{q_0} + \frac{1}{q_0 K_L} . \frac{1}{C_e} \quad (3)$$

$$\log q_e = \log K_f + \frac{1}{n} \log C_e \quad (4)$$

Where; q_e is the mass of adsorbate adsorbed for each mass of adsorbent (mg/g), C_e represents the concentration of the adsorbate at equilibrium (mg/L), q_0 and K_L the empirical constants relating to maximum adsorption capacity and free energy of adsorption respectively, K_f is the Freundlich capacity factor and n the Freundlich intensity parameter [33].

The mass of fluoride adsorbed for each unit mass of the adsorbent (q_e) in the dosage tests was computed using the mass balance equation (2). The quantity of fluoride adsorbed for each unit mass of WHAC (q_e) was plotted against the equilibrium fluorides concentration (C_e). Correlation coefficient (R^2) was used to establish the best fitting adsorption isotherm.

2.6. Adsorption Kinetics

Adsorption kinetics dictate the time required for the sorption reaction and are used to give crucial information on mechanisms of contaminant adsorption, thereby predicting adsorption rates applicable in design of adsorption systems [12, 47]. From the residual fluoride concentrations obtained in the adsorption tests at different contact times, phenomenological fluoride uptake q_t was determined by the mass balance expressed in equation (5).

$$q_t = \frac{(C_o - C_t)V}{m} \quad (5)$$

Where; q_t is the mass of fluoride adsorbed per unit mass of WHAC (mg/g) at time t, C_o and C_t represent fluoride quantities (mg/L) at time 0 and t (hours), V the volume of the water sample (liters), and m the mass of WHAC (g).

To understand the adsorption kinetics of fluorides on WHAC, the experimental data was fitted onto Pseudo-first and second order kinetic models as expressed in their linear forms in equations (6) and (7) respectively.

$$\ln(q_e - q_t) = \ln q_e - k_1 t \quad (6)$$

$$\frac{t}{q_t} = \frac{1}{q_e^2 k_2} + \frac{1}{q_e} t \quad (7)$$

Kinetic constants k_1 and q_e were determined from the slope and intercept of the graph of $\ln(q_e - q_t)$ against t following equation (6). Similarly, values for constants q_e and k_2 were determined from the slope and intercept of the plot of $\frac{t}{q_t}$ vs t respectively as per equation (7). The applicable kinetic model was determined by establishing the correlation factor, R^2 and comparing the q_e obtained from experiments and the theoretical q_e obtained from calculations [48].

3. Results and Discussions

3.1. Chemical Analysis of Groundwater Samples

The groundwater samples revealed an elevated fluoride concentration of 6.7 mg/L with a pH of 7.57 at 23ºC. The observed fluoride concentration exceeded both the WHO threshold of 1.5 mg/L and the Kenyan WASREB threshold of 3.0 mg/L for exceptional cases in drinking water. The results underscore the need for a defluoridation option to reduce associated fluoride risks.

3.2. Characterization of Water Hyacinth Activated Carbon

The test results for WHAC revealed critical physical and chemical parameters including functional groups present, moisture content, ash content, fixed carbon content, bulk density and surface homogeneity, which are significant in determining the suitability and efficiency of WHAC in defluoridation. The following sub-sections present the characterization results.

3.2.1. Proximate Analysis

Proximate analysis established a moisture content of 11.2%, ash content of 8.9% and volatile matter 13.2%, with the fixed carbon content computed as 66.7%. Table 1 compares the proximate analysis results of WHAC and selected CACs.

Table 1. *Proximate Analysis for WHAC against selected CACs.*

Type of Activated Carbon	Moisture Content (%)	Volatile matter (%)	Ash Content (%)	Fixed Carbon (%)	Reference
Water Hyacinth Activated Carbon (WHAC)	11.22	13.21	8.89	66.68	this study
Commercial Activated Carbon from EvaChem, Malysia	3.19	20.26	1.73	74.82	Mariah et al., 2023
Norit W35 commercial activated carbon from Cabot	2.40	4.62	8.7	84.27	Mestre et al., 2022

The characteristics of WHAC were closely aligned with the selected CAC's, with the ash content less than 10% and fixed carbon content greater than 65%. However, the departure in the moisture content of above 10% could be attributed to the impact of phosphoric acid used in the activation process. Generally, increased concentration of phosphoric acid leads to a rise in the number and volume of pores which in turn increases water absorption from the air [31]. The fixed carbon content gives an indication of the amount of carbon bound during pyrolysis after volatiles decompose. Fixed carbon proportions above 65% usually indicate good quality AC [4]. On the other hand, elevated ash contents indicate increased inactive sites, which reduce the active surface area of the AC and inhibits its adsorption capacity [29]. Based on the minimal moisture content, low ash content and high fixed carbon content, WHAC potentially has high surface area and porosity, which suggests that it is suitable for adsorption of fluorides in groundwater.

3.2.2. Bulk Density and pH

The pH and the bulk density for WHAC were 2.88 and 0.123 g/cm^3 respectively. The acidic pH can be attributed to the residual effect of concentrated phosphoric acid used in the activation process of WHAC preparation. Previous studies have reported the pH of CAC in the range of 6-7.3 [49]. The bulk density of 0.123 g/cm^3 was within the range for powdered activated carbons which have an average size of 20 microns, but below the range for granular CAC's which is between 0.25 and 0.45 g/cm^3. Generally, a high bulk density indicates more carbon in a given volume which translates to better adsorption. However, a much higher bulk density may also result in high pressure drop in the treatment system, which would slow down adsorption of the contaminant [23]. Based on its low bulk density, the WHAC had characteristics associated with ACs that are highly porous, easily regenerated and exhibiting fast adsorption kinetics.

3.2.3. FT-IR Characterization

Fourier Transform Infra-Red (FT-IR) Spectroscopy was used to establish the functional groups in WHAC. Absorbance and transmittance spectrums were generated from a wavenumber of 4000 to 500 cm^{-1}. Interpretation of the spectroscopy of WHAC depicted by the infra-red spectrum used the absorbance spectrum due to its linearity with the concentration of the absorbing substance. Additionally, it gives more precise peaks as opposed to the transmittance spectrum whose percent transmittance is exponential [37]. Figure 2 presents the absorbance spectrum of WHAC.

The peaks at 3388.49 and 3439.43 cm^{-1} are indicative of the O-H stretching vibration that is typically seen in the range of 3000 to 3600 cm^{-1}, and that is due to intermolecular hydrogen bonding of compounds like alcohols, phenols and carboxylic acids. The peaks may further indicate the presence of hydroxyl groups in the WHAC [20]. On the other hand, the weak peak between 3000 and 3300 cm^{-1} may indicate the existence of secondary amines with the N-H bond. The peak at 1651.43 cm^{-1} can be linked with stretching vibration of the C=C bond in the aromatic ring such as polycyclic aromatic hydrocarbons (PAHs) and phenols, while the peak at 1257.47 cm^{-1} can be linked with the C-O stretching vibration associated with the presence of ether or ester groups in the WHAC sample [36].

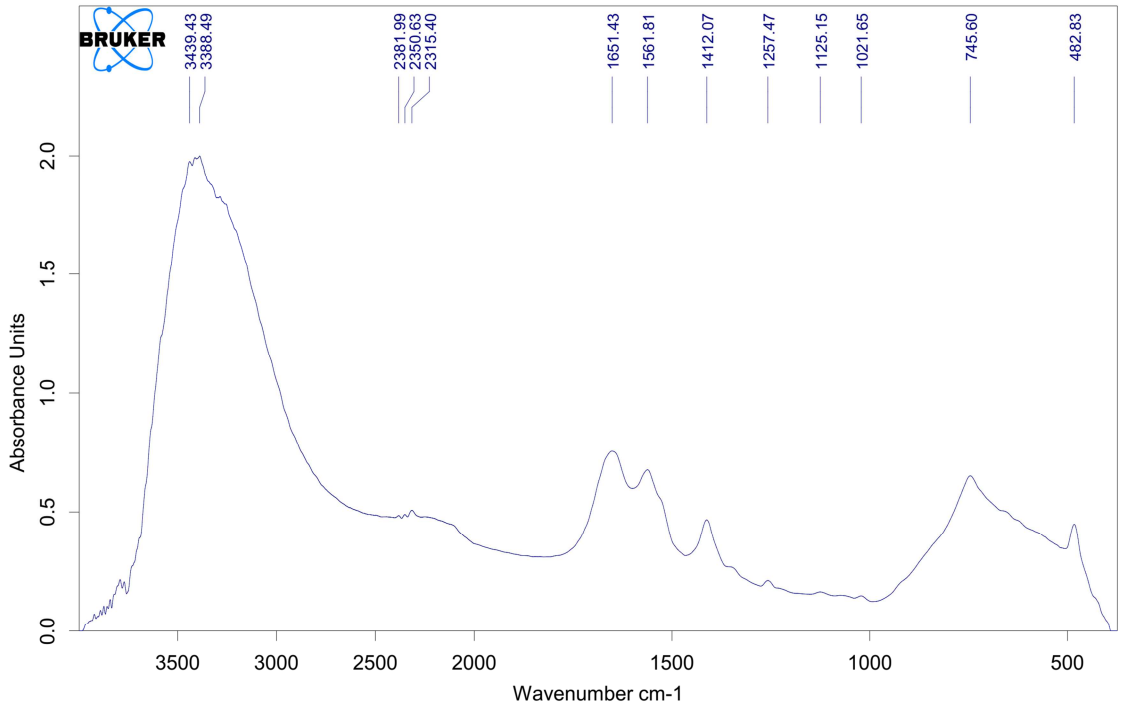

Figure 2. *FT-IR absorbance spectrum for WHAC.*

The presence of basic sites like hydroxyl and amine groups indicate WHAC's high potential for adsorption of fluorides as these chemical groups interact with fluoride ions through electrostatics, hydrogen bonding and complexation reactions [27]. Additionally, the presence of the aromatic C=C double bonds shows the potential application of WHAC in the adsorption of pesticides and herbicides, while the presence of hydroxyl groups indicates its potential for adsorption of heavy metals. Moreover, presence of ether or ester groups indicate potential for adsorption of phenols [27].

3.2.4. SEM Analysis

Micrographs from analysis of the Scanning Electron Microscopy (SEM) of the WHAC sample were used to provide information on the structure, surface morphology and composition. Figure 3 (a) and 3 (b) present the SEM micrographs of the WHAC at 300X and 800X magnification, respectively.

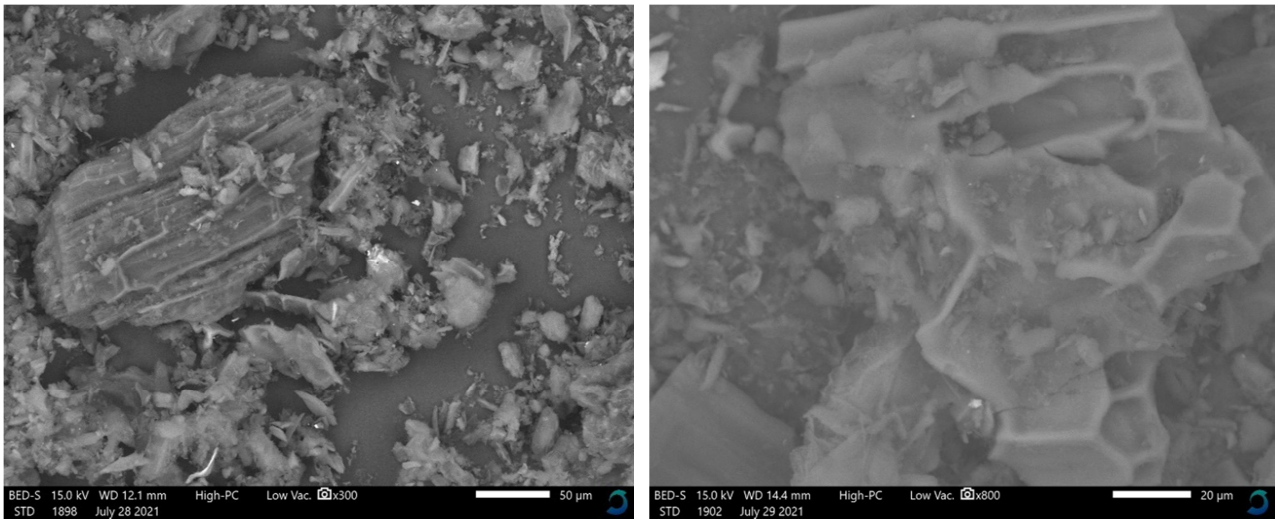

(a) (b)

Figure 3. *(a) WHAC micrograph at 300X, (b) WHAC micrograph at 800X.*

The SEM images revealed a rough and irregular surface texture with unevenly distributed particle sizes. Such properties reveal high porosity, a characteristic desired in an AC material. Additionally, the micrographs displayed an outer surface characterized by cavities and a honeycomb structure, signifying high surface area [46, 6]. Further, the images indicated that the pores were irregular and heterogenous and they were of different sizes.

3.3. Batch Defluoridation Studies

Batch experiments focused on determining the effect of pH, adsorbent concentration and duration of contact on defluoridation efficiency of WHAC.

3.3.1. Effect of pH

The defluoridation efficiency of WHAC was tested over a range of pH between 3 and 11 using 0.2 g WHAC /100 mL for 120 min. Table 2 depicts the results obtained from the tests.

Defluoridation efficiency of WHAC decreased with an increase in pH, with the highest efficiency achieved at pH 3. In the batch experiments, the adsorbent was mixed with the groundwater sample to form an electrically charged colloidal suspension. At low pH, hydrogen ions (H^+) in the solution made the WHAC surface more positive, increasing the electrostatic attraction of the negatively charged fluoride ions (F^-). However, in the alkaline media, the competition for active sites on the adsorbent between F^- and hydroxyl ions reduced the efficiency of the defluoridation [43] by a moderate 5.4%. The moderate effect of pH on defluoridation allows for operational efficiency in regard to pH.

Table 2. *Effect of pH on defluoridation efficiency of 0.2g/100 mL for 120 min.*

Groundwater pH	Initial Fluoride Concentration (mg/L)	Final Fluoride Concentration (mg/L)	Fluoride Removal Efficiency
3	6.7	1.70	74.6
5	6.7	1.80	73.1
7	6.7	1.93	71.1
9	6.7	1.97	70.7
11	6.7	2.07	69.2

3.3.2. Effect of Adsorbent Dosage

Batch tests were conducted using pH 3 to establish the effect of WHAC dosage on the efficiency of fluoride removal. Table 3 presents a summary of the test results on adsorbent dosage.

Table 3. *Effect of WHAC dosage on the defluoridation at 120 min contact and pH 3.*

WHAC Dosage in 100 mL of groundwater (g)	Initial Fluoride Concentration (mg/L)	Final Fluoride Concentration (mg/L)	Efficiency of Fluoride Removal %
0.2	6.7	1.67	75.1
0.4	6.7	1.53	77.1
0.6	6.7	1.43	78.6
0.8	6.7	1.30	80.6
1.2	6.7	1.17	82.6
1.6	6.7	1.17	82.6

The efficiency of fluoride removal increased from 75 to 82.6% with increase in WHAC dosage from 0.2 to 1.2 g. However, the defluoridation efficiency plateaued at 82.6% with a further increase of WHAC dosage to 1.6 g. Although increase in the adsorbent dosage, increased the surface area and sorption sites allowing for more fluoride particles to attach to the adsorbent, the adsorption rate reduced with the equilibrium fluoride concentration. The WHO limit for fluoride concentration of 1.5 mg/L was achieved with a WHAC dosage of about 0.4 g/100 mL.

3.3.3. Effect of Contact Time

Testing for the influence of contact duration on adsorption was conducted at pH of 3 and adsorbent dosage of 1.2 g, for a contact time ranging from 0 and 180 minutes. Figure 4 depicts the effect of contact time of WHAC with groundwater samples on the residual fluoride concentration.

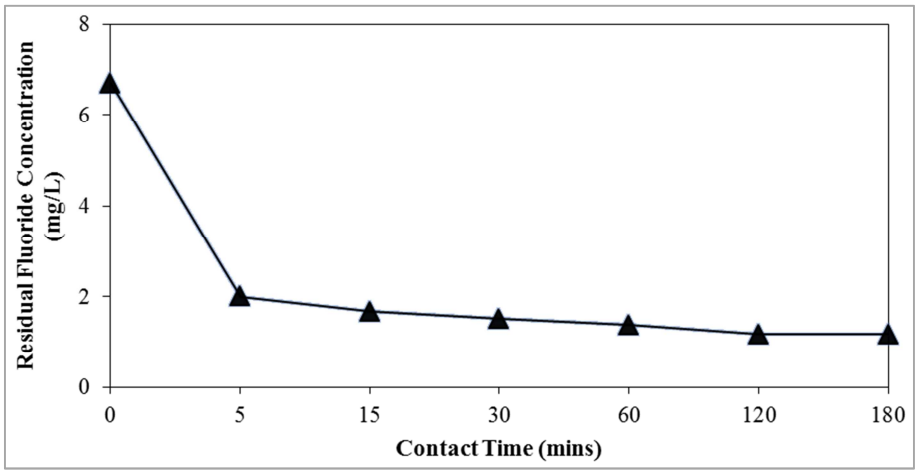

Figure 4. *Variation of residual fluoride concentration with contact time.*

The fluoride concentration decreased with increase in contact time up to 120 minutes. The first five minutes were characterized by high fluoride uptake attributed to readily available sorption sites in the AC, accounting for 90% of the total fluoride removed from the groundwater sample [43]. Between minutes 15 and 120, the removal rate slowed down, indicating intra-particle diffusion and adsorption in micro pores.

3.4. Adsorption Isotherm Modelling

The results of adsorption tests were modelled with the Langmuir and Freundlich isotherms for WHAC dosages 0.2 to 1.6 g in 100 ml groundwater sample, initial fluoride concentration (C_o) 6.7 mg/L and a contact time 120 minutes. Table 4 presents the equilibrium concentrations (C_e) and adsorption capacity q_e, obtained for each WHAC dosage.

Table 4. *Equilibrium fluoride concentrations at different WHAC dosage.*

WHAC Dosage (g) in 100 mL of ground water	C_o (mg/L)	C_e (mg/L	q_e (mg/g)
0.2	6.7	1.67	2.517
0.4	6.7	1.53	1.292
0.6	6.7	1.43	0.878
0.8	6.7	1.30	0.675
1.2	6.7	1.17	0.461
1.6	6.7	1.17	0.346

The equilibrium data from the experiment was fitted in the Freundlich and Langmuir isotherm models as presented in following sub-sections.

3.4.1. Freundlich Isotherm

A plot of Log q_e against Log C_e was used to generate the Freundlich adsorption isotherm depicted in figure 5.

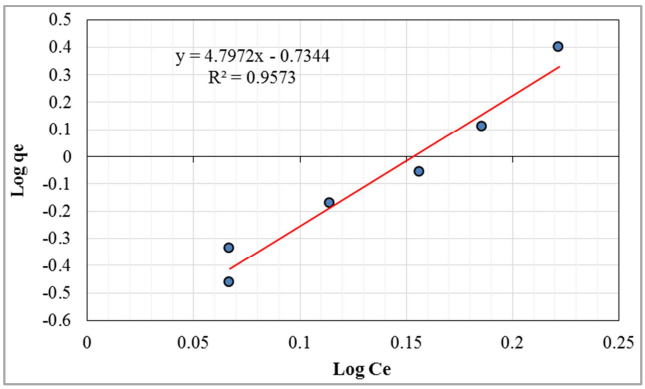

Figure 5. *Freundlich isotherm for adsorption of fluorides on WHAC.*

The equilibrium adsorption data demonstrated a good fit to the Freundlich isotherm model yielding a correlation factor (R^2) of 0.9573 and a slope 1/n of 4.80. 1/n is indicative of the adsorption intensity and surface heterogeneity of the adsorbent. When n = 1, adsorption is homogenous and all adsorption sites on the adsorbent's surface exhibit the same affinity for the adsorbate. When n < 1, the adsorption is favorable while when n > 1 the adsorption is unfavorable. For the observed n (0.2085) < 1, adsorption of fluorides on WHAC was favorable, which indicates that the adsorption sites on WHAC are heterogenous and have a high affinity to fluorides. Additionally, the 1/n (4.7972) > 1 denoted, adsorption of fluorides on WHAC was cooperative indicating that already adsorbed fluoride molecules positively influenced the adsorption of "new" fluoride ions. The Freundlich capacity factor K_f, was 0.1843; generally, a large Freundlich factor indicates large affinity of the adsorbent for the adsorbate.

3.4.2. Langmuir Isotherm

The experimental equilibrium data were also modeled with the Langmuir isotherm with the linearized equation (3). Figure 6 depicts the plot of $1/q_e$ against $1/C_e$.

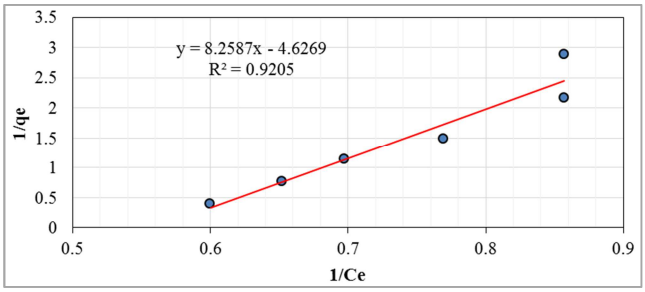

Figure 6. *Langmuir isotherm for adsorption of fluorides on WHAC.*

The Langmuir adsorption model provided a good fit to the experimental data yielding a correlation coefficient (R^2) value of 0.9205, which was lower than that for the Freundlich isotherm. The result showed that the model only partially described the adsorption of fluorides onto WHAC. The Langmuir model presumes homogeneity of the adsorbent's sites and that the adsorption process is monolayer. Therefore, it can be concluded that adsorption sites of WHAC are heterogeneous. This result is consistent with conclusions made from the Freundlich adsorption model. The observation that WHAC is heterogeneous is also consistent with the SEM images that indicated that WHAC surface is rough and heterogenous.

3.5. Adsorption Kinetics

Adsorption kinetics mathematically describe the rate of adsorption and are used to estimate the time required to attain equilibrium, the adsorption capacity of an adsorbent and the rate at which the adsorbent can remove an adsorbate from a solution. Adsorption kinetics studies were conducted by exposing 100 ml of the groundwater sample with 6.7 mg/L fluoride concentration to 1.2 g of WHAC for a contact time ranging between 5 to 180 minutes. The experimental data acquired from batch tests were fitted to pseudo-first order and pseudo-second order kinetic models.

3.5.1. Pseudo-First Order Kinetic Model

The linearized first order kinetic equation (6) was applied and a graph of ln (q_e-q_t) vs t was plotted. Figure 7 shows the plot of the pseudo-first order kinetic model.

The experimental data was only partially described by the pseudo-first order kinetic model with a correlation coefficient (R^2) of 0.9175. From the plot, the rate constant K_1 was tabulated as 0.0272 min^{-1}. On the other hand, the theoretical q_e calculated from the plot was 0.0662 mg/g which differs significantly from the experimental q_e which was 0.4608 mg/g. Based on this significant difference between the theoretical and experimental q_e, it was concluded that adsorption of fluorides on WHAC did not conform to pseudo-first order kinetic model.

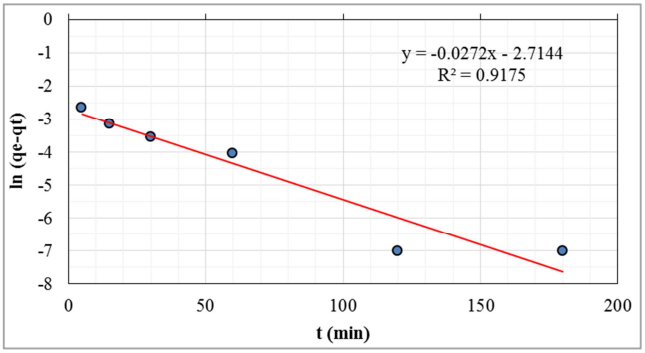

Figure 7. *Pseudo-first order kinetic model for adsorption of fluorides onto WHAC.*

3.5.2. Pseudo-Second Order Kinetic Model

The linearized second order kinetic equation (7) was applied and a graph of t/q_t vs t was plotted. Figure 8 shows the plot of the pseudo-second order kinetic model.

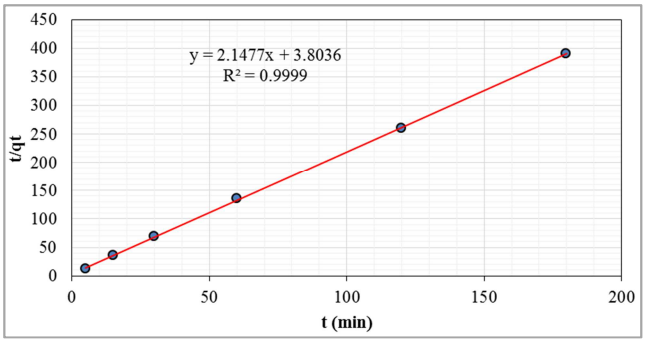

Figure 8. *Pseudo-second order kinetic model for adsorption of fluorides onto WHAC.*

The experimental data exhibited a strong fit to the pseudo-second order kinetic model with a correlation factor (R^2) of 0.9999. The rate constant K_2 was tabulated as 1.2128 min^{-1} while the theoretical q_e calculated from the plot was 0.4656 mg/g. This closely matches with the experimental q_e of 0.4608, showing that adsorption of fluorides onto WHAC conforms to the pseudo-second order kinetic model. From this finding, it was concluded that adsorption of fluorides by WHAC was predominantly by chemisorption involving the establishment of chemical bonds between fluorides and WHAC and that the rate-limiting step in the adsorption process was the chemical reaction between fluorides and WHAC [2].

Table 5. *Pseudo-first order and pseudo-second order kinetic model constants for adsorption of fluorides onto WHAC.*

Kinetic model	R^2	K_1/ K_2 (1/min)	q_e (experimental) (mg/g)	q_e (calculated) (mg/g)
Pseudo-first order	0.9175	0.0272	0.4608	0.0662
Pseudo-second order	0.9999	1.2128	0.4608	0.4656

Table 5 summarizes the constants obtained in pseudo-first order and pseudo-second order kinetic models.

4. Conclusion

The study show that WHAC presents a cost-effective option for defluoridation of groundwater in decentralized systems of developing countries. The characteristics of WHAC compared closely with two selected CACs namely, biomass-based Norit W35 and CAC from EvaChem with ash content of less than 10% and fixed carbon content above 65% suggesting that water hyacinth is a suitable precursor for activated carbon. Defluoridation of groundwater with the WHAC reduced fluoride concentration in the groundwater from 6.7 to 1.17 mg/L, which was within WHO's drinking water threshold of 1.5 mg/L. The pH of water samples has a moderate effect on defluoridation efficiency with an increase of 5.4% for pH change from pH 11 to 3. The defluoridation efficiency increased with WHAC dosage from 0.2 to 1.2 g WHAC/100 mL from 75.1 to 82.6% with 68% efficiency achieved in first 5 minutes. The adsorption of fluoride on WHAC conformed to the Freundlich isotherm model indicating that it is heterogeneous. Additionally, the adsorption conformed to the pseudo-second order kinetic model with a correlation factor of 0.9999 compared to 0.9175 for the pseudo-first order kinetic model, suggesting that the process was predominantly chemisorption. The study recommends further research to establish the scalability of defluoridation with WHAC for continuous flow.

Conflict of Interest

The authors declare that they have no competing interests.

References

[1] Anisuzzaman, S. M., Joseph, C. G., Taufiq-Yap, Y. H., Krishnaiah, D., & Tay, V. V. (2015). Modification of commercial activated carbon for the removal of 2,4-dichlorophenol from simulated wastewater. *Journal of King Saud University - Science*, *27* (4), 318–330.

[2] Aslam, M. M. A., Kuo, H.-W., Den, W., Sultan, M., Rasool, K., & Bilal, M. (2022). Chapter 10—Recent trends of carbon nanotubes and chitosan composites for hexavalent chromium removal from aqueous samples. In S. Ahuja (Ed.), *Separation Science and Technology* (Vol. 15, pp. 177–207). Academic Press. https://doi.org/10.1016/B978-0-323-90763-7.00006-8

[3] Bansal, R. C., & Goyal, M. (2005). Activated carbon adsorption. *Taylor & Francis*.

[4] Budianto, A., Kusdarini, E., Effendi, S. S. W., & Aziz, M. (2019). The Production of activated carbon from Indonesian mangrove charcoal. *IOP Conference Series: Materials Science and Engineering*, *462*, 012006. https://doi.org/10.1088/1757-899X/462/1/012006

[5] CCEFW. (2010). Excess fluoride in water: report of the consultative committee Kenya Bureau of Standards. *KeBS*.

[6] Cherono, F., Mburu, N., & Kakoi, B. (2021). Adsorption of lead, copper and zinc in a multi-metal aqueous solution by waste rubber tires for the design of single batch adsorber. *Heliyon*, *7* (11), e08254. https://doi.org/10.1016/j.heliyon.2021.e08254

[7] Deetae, P., & Wongpromrat, P. (2019). Study of atrazine adsorption kinetics by using an activated carbon synthesised from water hyacinth. *E3S Web of Conferences*, *116*.

[8] Dickinson, R., & Royer, F. (2014). Weeds of North America. *University of Chicago Press*.

[9] Doczekalska, B., Bartkowiak, M., Orszulak, G., & Katolik, Z. (2015). Activated carbon from plant materials. *Ann. WULS - SGGW, For. and Wood Technol.*, *92*, 88–91.

[10] Doczekalska, B., Bartkowiak, M., Waliszewska, B., Orszulak, G., Cerazy-Waliszewska, J., & Pniewski, T. (2020). Characterization of chemically activated carbons prepared from miscanthus and switchgrass biomass. *Materials*, *13* (7), 1654.

[11] Elazab, H., & Ibrahim, K. (2019). Methylene blue removal using water hyacinth derived active carbon. *Lambert Academic Publishing*.

[12] Emmanuel, K. A., Ramaraju, K. A., Rambabu, G., & Rao, A. V. (2008). Removal of fluoride from drinking water with activated carbons prepared from HNO_3 activation—a comparative study. *Rasayan J. Chem.*, *1* (4), 802–818.

[13] Fawell, Bailey, K., Chilton, J., Dahi, E., Fewtrell, L., & Magara, Y. (Eds.). (2006). Fluoride in drinking-water. *IWA Pub*.

[14] Gaurav, G. K., Mehmood, T., Cheng, L., Klemeš, J. J., & Shrivastava, D. K. (2020). Water hyacinth as a biomass: A review. *Journal of Cleaner Production*, 122214.

[15] Gayathri, G., Raju, K., Dinesh, S., & Beulah, M. (2017). Defluoridation of groundwater using low cost adsorbents.pdf. *International Journal of Earth Sciences and Engineering*, *10* (5).

[16] Gevera, P., Mouri, H., & Maronga, G. (2018). High fluoride and dental fluorosis prevalence: A case study from Nakuru area, The Kenyan Rift Valley. *EGU General Assembly Conference Abstracts*, 1422.

[17] Habuda-Stanić, M., Ravančić, M., & Flanagan, A. (2014). A Review on Adsorption of Fluoride from Aqueous Solution. *Materials*, *7* (9), 6317–6366.

[18] Isichei, T., & Okieimen, Felix. (2014). Adsorption of 2-Nitrophenol onto water hyacinth activated carbon-kinetics and equilibrium studies. *Environment and Pollution*, *3* (4), p99.

[19] Johnson, P. J., Setsuda, D. J., & Williams, R. S. (1999). Activated carbon for automotive applications. *Carbon Materials for Advanced Technologies* (pp. 235–268). Elsevier. https://doi.org/10.1016/B978-008042683-9/50010-8

[20] Joshi, S., & Pokharel, B. P. (2014). Preparation and characterization of activated carbon from Lapsi (Choerospondias axillaris) seed stone by chemical activation with potassium hydroxide. *Journal of the Institute of Engineering*, *9* (1), 79–88. https://doi.org/10.3126/jie.v9i1.10673

[21] Kahama, R. W., Kariuki, D. N., Kariuki, H. N., & Njenga, L. W. (1997). Fluorosis in children and sources of fluoride around Lake Elementaita region of Kenya. *Fluoride*, *30* (1), 19–25.

[22] KNBS. (2019). Kenya housing and population census: Volume iv; distribution of population by socio-economic characteristics. *Government of Kenya.*

[23] Koehlert, K. (2017). Activated carbon: Fundamentals and new applications. *Cabot Corp.*

[24] Kut, K. M. K., Sarswat, A., Srivastava, A., Pittman, C. U., & Mohan, D. (2016). A review of fluoride in African groundwater and local remediation methods. *Groundwater for Sustainable Development*, *2* (3), 190–212.

[25] Kwiatkowski, J. F. (Ed.). (2012). Activated carbon: classifications, properties and applications. *Nova Science Publishers.*

[26] Mahamadi C. (2012). Water hyacinth as a biosorbent: A review. *African Journal of Environmental Science and Technology*, *5* (13).

[27] Manikannan, K., Abraham, M. K., Karthick Raja Namasivayam, S., Raji, V. R., Raj, S., & Moovendhan, M. (2022). Removal of fluoride from water by natural biosorbents and evaluation of microstructure and functional groups in removal process. *Biomass Conversion and Biorefinery*. https://doi.org/10.1007/s13399-022-03588-6

[28] Mariah, M. A. A., Rovina, K., Vonnie, J. M., & Erna, K. H. (2023). Characterization of activated carbon from waste tea (Camellia sinensis) using chemical activation for removal of methylene blue and cadmium ions. *South African Journal of Chemical Engineering*, *44*, 113–122. https://doi.org/10.1016/j.sajce.2023.01.007

[29] Martínez-Mendoza, K. L., Barraza Burgos, J. M., Marriaga-Cabrales, N., Machuca-Martinez, F., Barajas, M., & Romero, M. (2020). Production and characterization of activated carbon from coal for gold adsorption in cyanide solutions. *Ingeniería e Investigación*, *40* (1), 34–44. https://doi.org/10.15446/ing.investig.v40n1.80126

[30] Marwa, J., Lufingo, M., Noubactep, C., & Machunda, R. (2018). Defeating fluorosis in the east African rift valley: transforming the Kilimanjaro into a rainwater harvesting park. *Sustainability*, *10* (11), 4194.

[31] Maulina, S., & Iriansyah, M. (2018). Characteristics of activated carbon resulted from pyrolysis of the oil palm fronds powder. *IOP Conference Series: Materials Science and Engineering*, *309*, 012072. https://doi.org/10.1088/1757-899X/309/1/012072

[32] Mestre, A. S., Viegas, R. M. C., Mesquita, E., Rosa, M. J., & Carvalho, A. P. (2022). Engineered pine nut shell derived activated carbons for improved removal of recalcitrant pharmaceuticals in urban wastewater treatment. *Journal of Hazardous Materials*, *437*, 129319. https://doi.org/10.1016/j.jhazmat.2022.129319

[33] Metcalf & Eddy. (2002). Wastewater engineering: treatment and reuse (G. Tchobanoglous & H. D. Stensel, Eds.). *McGraw-Hill Education*.

[34] Mobeen, N., & Kumar, P. (2017). Defluoridation techniques—a critical review. *Asian Journal of Pharmaceutical and Clinical Research*, *10* (6), 64.

[35] Mohapatra, M., Anand, S., Mishra, B. K., Giles, D. E., & Singh, P. (2009). Review of fluoride removal from drinking water. *Journal of Environmental Management*, *91* (1), 67–77.

[36] Nandiyanto, A., Oktiani, R., & Ragadhita, R. (2019). How to Read and Interpret FTIR Spectroscope of Organic Material. *Indonesian Journal of Science and Technology*, *4*, 97–118. https://doi.org/10.17509/ijost.v4i1.15806

[37] Nipun. (2015, August 3). Difference between absorbance and transmittance. Pediaa.Com. Retrieved March 22, 2023, from https://pediaa.com/difference-between-absorbance-and-transmittance/

[38] Omondi, E. A., Ndiba, P. K., & Njuru, P. G. (2019). Characterization of water hyacinth (E. crassipes) from Lake Victoria and ruminal slaughterhouse waste as co-substrates in biogas production. *SN Applied Sciences*, *1* (8), 848.

[39] Omondi, E. A., Ndiba, P. K., Chepkoech, K., & Kegode, A. (2023). Modeling anaerobic co-digestion of water hyacinth with ruminal slaughterhouse waste for first order, modified gompertz and logistic kinetic models. *International Journal of Renewable Energy Research*, *12*, 569–580. https://doi.org/10.14710/ijred.2023.52775

[40] Patil, S., & Ingole, N. (2012). Studies on defluoridation: A critical review. *Journal of Engineering Research and Studies*.

[41] Petersen-Perlman, J., Megdal, S., Gerlak, A., Wireman, M., Zuniga-Teran, A., & Varady, R. (2018). Critical issues affecting groundwater quality governance and management in the United States. *Water*, *10* (6), 735. https://doi.org/10.3390/w10060735

[42] Poudyal, M. (2015). Investigation on the efficiencies of low-cost adsorbents for the treatment of fluoride contaminated water. *Kathmadu University Press.*

[43] Poudyal, M., & Babel, S. (2015). Removal of fluoride using granular activated carbon and domestic sewage sludge. *International Conference on Informatics, Environment, Energy and Application*, *82*.

[44] Riyanto, C. A., & Prabalaras, E. (2019). The adsorption kinetics and isoterm of activated carbon from water hyacinth leaves (Eichhornia crassipes) on Co(II). *Journal of Physics: Conference Series*, *1307* (012002).

[45] Salifu, A. (2017). Fluoride removal from groundwater by adsorption technology: the occurrence, adsorbent synthesis, regeneration and disposal (1st ed.). *CRC Press.*

[46] Tarapitakcheevin, P., Weerayutsil, P., & Khuanmar, K. (2013). Adsorption of acid dye on activated carbon prepared from water hyacinth by sodium chloride activation. *GMSARN International Journal, 7* (2013), 83-90.

[47] Telkapalliwar, N. G., & Shivankar, V. M. (2019). Data of characterization and adsorption of fluoride from aqueous solution by using modified Azadirachta indica bark. *Data in Brief*, *26*, 104509.

[48] Uddin, M. T., Islam, M. S., & Abedin, M. Z. (2007). Adsorption of phenol from aqueous solution by water hyacinth ash. *ARPN Journal of Engineering and Applied Sciences*, *2* (2), 11–17.

[49] Vojnović, B., Cetina, M., Franjković, P., & Sutlović, A. (2022). Influence of initial pH value on the adsorption of reactive black 5 dye on powdered activated carbon: kinetics, mechanisms, and thermodynamics. *Molecules*, *27* (4). https://doi.org/10.3390/molecules27041349

[50] Wambu, E. W., & Muthakia, G. (2011). High fluoride water in the Gilgil area of Nakuru County, Kenya. *Fluoride*, *44* (1), 37–41.

[51] WASREB. (2016). Drinking water quality and effluent monitoring guideline. *Water Services Regulatory Board.*

[52] WHO. (2017). Guidelines for drinking-water quality (4th ed + 1st add). *World Health Organization*.

[53] Yakout, S. M., & El-Deen, S. (2016). Characterization of activated carbon by phosphoric acid activation of olive stones. *Aranian Journal of Chemistry*, *9*, 1155–1162.

[54] Yapo, N. S., Aw, S., Briton, B. G. H., Drogui, P., Yao, K. B., & Adouby, K. (2022). Removal of fluoride in groundwater by adsorption using hydroxyapatite modified Corbula trigona shell powder. *Chemical Engineering Journal Advances*, *12*, 100386. https://doi.org/10.1016/j.ceja.2022.100386